

Article

Immunotherapeutic Development of a Tri-Specific NK Cell Engager Recognizing BCMA

Felix Oh ¹, Martin Felices ², Behiye Kodal ², Jeffrey S. Miller ² and Daniel A. Vallera ^{1,*} 

¹ Department of Radiation Oncology, Laboratory of Molecular Cancer Therapeutics, University of Minnesota Masonic Cancer Center, Minneapolis, MN 55455, USA; felixoh99@gmail.com

² Department of Medicine, Division of Hematology, Oncology, and Transplantation, University of Minnesota Masonic Cancer Center, Minneapolis, MN 55455, USA; mfelices@umn.edu (M.F.); mille011@tc.umn.edu (J.S.M.)

* Correspondence: valle001@umn.edu

Simple Summary: Chemotherapy-refractory multiple myeloma (MM) is serious and life-threatening, and better treatments are urgently needed. BCMA is a cell surface protein known to be expressed on MM and therefore an accepted target for antibody therapy, but progress has been slow. Natural killer (NK) cells normally fend off cancer cells, but many cancers override them. Using a more aggressive strategy, we bioengineer a tri-specific biological drug containing an antibody fragment that binds BCMA, an antibody fragment that binds NK cells, as well as an NK-enhancing cytokine. Together, this complex triggers a more robust NK response. Studies in test tubes show that the hybrid drug enhances NK expansion, priming, and activity against MM cell lines. Importantly, studies in special immunosuppressed mice receiving lethal doses of human MM cells show anti-cancer activity. Studies indicate that the drug should be considered further for clinical development.

Abstract: Chemotherapy-refractory multiple myeloma (MM) is serious and life-threatening, and better treatments are urgently needed. BCMA is a prominent marker on the cell surface of MM cells, rendering it an accepted target for antibody therapy. Considering that MM is a liquid tumor and immunotherapy has enjoyed success against leukemia, we devise an approach designed to enhance NK cell activity against MM. Ordinarily, NK cells function to naturally survey the body and eliminate malignant cells. Our platform approach is designed to enhance NK function. A tri-specific immune-engaging TriKE is manufactured, consisting of a camelid nanobody VHH antibody fragment recognizing CD16 expressed on NK cells and an scFv antibody fragment specifically recognizing BCMA. These two fragments are crosslinked by the human cytokine interleukin-15 (IL-15) known to have prominent activating effects on NK cells. The molecule, when tested by flow cytometry, shows activation of NK cells in their numbers and activity. Additionally, the molecule demonstrates anti-cancer effects in an in vivo xenograft model of human MM. We believe that the drug will have the capability of enhancing NK cells at the site of the immune synapse, i.e., the effector:target cell interface, and this will promote cancer remissions.

Keywords: NK cells; BCMA; ADCC; IL-15; bispecific antibodies; multiple myeloma; innate immunotherapy; TriKEs; leukemia; lymphoma



Citation: Oh, F.; Felices, M.; Kodal, B.; Miller, J.S.; Vallera, D.A.

Immunotherapeutic Development of a Tri-Specific NK Cell Engager Recognizing BCMA. *Immuno* **2023**, *3*, 237–249. <https://doi.org/10.3390/immuno3020016>

Academic Editor: Alessandra Fierabracci

Received: 15 March 2023

Revised: 26 May 2023

Accepted: 15 June 2023

Published: 20 June 2023



Copyright: © 2023 by the authors. Licensee MDPI, Basel, Switzerland. This article is an open access article distributed under the terms and conditions of the Creative Commons Attribution (CC BY) license (<https://creativecommons.org/licenses/by/4.0/>).

1. Introduction

Multiple myeloma (MM) is a liquid cancer of the plasma cells with a poor prognosis, often culminating in bone marrow failure, anemia, immune paresis, infection, bone fractures, bone pain, high calcium levels, and renal failure [1]. Combination therapies incorporating proteasome inhibitors, antibodies, and histone deacetylase inhibitors have extended survival rates [2–4]. However, most patients still die with cancer recurrence due to minimal residual disease (MRD), and MM remains an incurable disease for the

majority of patients [5]. Though complete eradication of the disease is almost impossible to achieve, current therapeutics are aimed at effectively managing disease progression. A predominant marker expressed on MM cells is B-cell maturation antigen (BCMA). BCMA, also known as TNFRSF17 or CD269, is a member of the tumor necrosis factor receptor (TNFR) superfamily [6]. Preferentially expressed on mature B cells, BCMA is integrally associated with MM as a biomarker and therapeutic target. BCMA is expressed on the surface of nearly all MM cell lines. It is more abundantly present in malignant plasma cells than normal plasma cells [7,8]. Investigators have shown that BCMA overexpression promotes *in vivo* growth of xenografted MM cells in murine models [9]. Upregulated during MM pathogenesis [10], higher BCMA expression levels are associated with poorer outcomes, emphasizing its role as a useful biomarker of MM prognosis [11]. The importance of BCMA as a therapeutic target is demonstrated by over 40 clinical trials targeting BCMA that are currently recruiting and listed on the [Clinicaltrials.gov](https://clinicaltrials.gov) website (accessed on 15 March 2023). These include antibodies, BCMA-recognizing car T cells, and bispecific antibodies.

Recent advances in immunotherapy, focusing mostly on T cell-engaging agents, offer encouragement. However, T cell approaches present with certain adverse risks associated with T cell targeting including severe cytokine toxicity and neurotoxicity [12,13]. Natural killer cell (NK cell) therapies are currently under consideration as alternative treatments due to their lack of MHC restriction and immunogenicity [14]. NK cells are powerful mediators of the innate immune system that can mediate unselective killing of tumors through natural cytotoxicity and can selectively kill cancer cells through antibody-dependent cell-mediated cytotoxicity (ADCC). ADCC occurs when NK cells, through the receptor CD16 (or Fc γ RIII), bind the Fc portion of antibodies bound to cancer cells. This triggers NK cell activation, in the form of calcium flux and phosphorylation of immunoreceptor tyrosine-based activation motif (ITAMS), culminating in the directional release of enzymes perforin and granzyme, which mediates tumor lysis, and inflammatory cytokines IFN γ and TNF α [15–17]. To model this natural process, we bio-engineered a single-chain protein composed of anti-BCMA scFv (single-chain variable fragment) antibody fragment reactive with MM cells and a humanized anti-CD16 single-domain antibody (sdAb) derived from a camelid. These camelid antibodies are called nanobodies [18] and are found to improve the refolding and NK activation of our drug [19–21]. Our contribution to the platform is the addition of modified human IL-15 cross-linker to enhance survival and expansion of human NK cells. These trispecific NK cell engagers are called TriKEs and could be generated against a variety of cancer cell targets [22,23]. Mechanistically, we believe that the anti-CD16 and the anti-BCMA moieties facilitate formation of a synapse between NK cells and MM cells resulting in high levels of antibody-dependent cell-mediated cytotoxicity (mechanism illustrated in Supplemental Figure S1). The human IL-15 incorporated into our drug enhances NK cell activation and expansion, providing even more effector cells at the tumor site.

IL-15 is critical in NK cell development, affecting homeostasis, proliferation, survival, and activation [24]. IL-15 is an inflammatory cytokine. Its prevailing mechanism of action is juxtacrine signaling and trans-presentation mediated by membrane-bound complex IL-15/IL-15R α [15]. The signaling pathway of IL-15 begins with binding to an IL-15R α receptor, with subsequent presentation to surrounding NK cells bearing IL-15R $\beta\gamma$ c complex on their cell surface. NK cells have relatively short half-lives in circulation and naturally slow proliferation rates which necessitate IL-15 stimulation following NK activation [25,26]. Key factors in choosing IL-15 are its preference for NK cell reactivity and the fact that it does not stimulate Tregs, which is known to shut down immune response [27]. In contrast, IL-2, a well-studied immunotherapeutic cytokine, does stimulate Tregs. Studies also suggest that the toxicity profiles of IL-15 may be more favorable than those of IL-2 [28].

In this paper, we examine the potential of an anti-MM NK-engaging TriKE to kill MM target cells *in vitro* and also in a xenogeneic mouse model in which enriched human NK cells and MM cells are both present.

2. Materials and Methods

2.1. Construction and Purification of cam1615BCMA

A second generation anti-BCMA NK engager was created, called cam1615BCMA or TriKE[®]. The n-terminus consisted of a single-chain VHH camelid fragment recognizing CD16 [29] with downstream human IL-15, and then a downstream humanized BCMA scFv antibody fragment [30]. The camelid VHH was included since the advantages over conventional scFv and the final product had enhanced purity and yield in our bacterial expression system [19]. Once a camelid sequence was identified, it was spliced into a universal humanized nanobody scaffold designed to accommodate antigen binding loops maintaining antibody affinity and specificity [31]. Importantly, upstream PSGQAGAAASESLFVSNHAY and downstream EASGGPE flanking sequences were used for molecular alignment. The assembled target gene was 1545 base pairs. The final sequence was confirmed by the University of Minnesota Biomedical Genomics Center core facility.

The protein was expressed in *Escherichia coli* strain Rosetta (DE3) (Novagen, Madison, WI, USA) after plasmid transfection. Bacteria were cultured in Luria broth with 50 µg/mL kanamycin, and IPTG (GoldBio, Saint Louis, MO, USA) was used to trigger expansion. Bacterial expression in this manner mostly results in the sequestration of protein in inclusion bodies (IB), dense electron-refractile particles of the aggregated protein. This necessitates IB homogenization (buffer: 50 mM Tris, 50 mM NaCl, and 5 mM EDTA pH 8.0) sonication, and centrifugation to obtain pellets. The protein was extracted in 0.3% sodium deoxycholate, 5% Triton X-100, 10% glycerin, 50 mmol/L Tris, 50 mmol/L NaCl, and 5 mmol/L EDTA (pH 8.0) and washed. To regain tertiary conformation, the protein was then refolded using a sodium N-lauroyl-sarcosine (SLS) air oxidation method modified from a previously reported procedure [32].

Upon completion of the refolding step, the product was dialyzed against 5 volumes of 20 mM Tris-HCl at pH 8.0 for 48 h at 4 °C, then 8 volumes for 18 additional hours. The final solution was then purified in two orthogonal column steps using fast flow Q ion exchange chromatography and then size-exclusion chromatography (Superdex 200, GE). Sodium dodecyl sulfate polyacrylamide gel electrophoresis (SDS-PAGE) analysis with Simply Blue Safe Stain (Invitrogen, Carlsbad, CA, USA) was used to verify the final purity and size.

2.2. Cell Lines and Blood and Human Blood

All cell lines were obtained from the American Type Culture Collection: MM.1S (ATCC[®] CRL-2974[™]) was obtained from the parent line MM.1, established from the blood of a multiple myeloma patient resistant to steroid-based therapy. Lines U266 (ATCC[®] TIB-196[™]) and RPMI 8226 (ATCC[®] CRM-CCL-155[™]) were also derived from multiple myeloma patients. Lines were grown in RPMI 1640 (with 10–20% fetal bovine serum and 2 mmol/L L-glutamine and incubated at 5% CO₂, 37 °C). Cells with viabilities greater than 95% were used in experiments.

Peripheral blood mononuclear cells (PBMCs) from the blood of de-identified healthy donors were obtained, after participants gave informed consent, from Memorial Blood Centers (Minneapolis, MN, USA) and used in compliance with the Committee on the Use of Human Subjects in Research (IRB# 9709M00134) and in accordance with the Declaration of Helsinki. Cells were isolated using density-gradient centrifugation with Ficoll-Paque Premium.

2.3. Evaluation of NK Cell Activity

To evaluate NK cell activity, we used a flow cytometric assay that measures NK cell degranulation and inflammatory cytokine production. The assay utilizes flow cytometry to measure LAMP-1 (CD107a) expressed on the surface of activated effector cell membranes following effector cell attack and target cell lysis [33]. Extensive studies show that the assay correlates well with conventional Cr-51 isotope release assay data [34]. Briefly, PBMCs were incubated overnight in RPMI 1640 (supplemented with 10% FCS) with tumor targets. Drugs were then added to facilitate ADCC for 10 min at 37 °C. Fluorescein isothiocyanate (FITC)-conjugated anti-human CD107a monoclonal antibody (BD Biosciences, Franklin Lakes, NJ, USA) was then added for

1 h. GolgiStop (1:1500, BD Biosciences, Franklin Lakes, NJ, USA) and GolgiPlug (1:1000, BD Biosciences, Franklin Lakes, NJ, USA) was then added, and cells were incubated for an additional 3 h at 37 °C, 5% CO₂. Cells were then washed and stained for 15 min at 4 °C. Staining agents included PE/Cy 7-conjugated anti-CD56 mAb, APC/Cy 7-conjugated anti-CD16 mAb, and PE-CF594-conjugated anti-CD3 mAb (BD Biosciences, Franklin Lakes, NJ, USA). Finally, cells were washed and fixed (2% paraformaldehyde). Cells were then permeabilized with a commercial solution (BD Biosciences, Franklin Lakes, NJ, USA) and incubated with Pacific Blue-conjugated anti-human IFN γ (BioLegend, San Diego, CA, USA) for 20 min. Cells were then washed and analyzed using flow cytometry (LSRII flow cytometer, BD Biosciences, Franklin Lakes, NJ, USA) gating on CD56+CD3⁻ cells defining the NK cell population. Data analysis was performed with FlowJo software (FlowJo Enterprise LCC, version 7.6.5, Ashland, OR, USA). Our gating strategy is depicted in Supplemental Figure S2.

Cytotoxicity was evaluated by 4-h ⁵¹Cr-release assays. Briefly, resting PBMC from normal donors treated with 30 nM drug or control agents were cocultured for 4 h with ⁵¹Cr-labeled MM.1S targets at varying E:T ratios. PBMCs cells were cocultured with targets at a 20:1 (E:T) ratio in the presence of 30 nmol/L TriKE. ⁵¹Cr release was measured by a gamma scintillation counter (Perkin Elmer, Waltham, MA, USA), and specific target lysis was determined.

2.4. NK Cell Expansion via IL-15 Stimulation

To measure the functionality of our IL-15 cross-linker, PBMCs or enriched NK cells from healthy donors were labeled with CellTrace Violet Proliferation Dye (Invitrogen, Carlsbad, CA, USA) according to kit instructions. Cells were cultured with 50 nM TriKE or controls (5% CO₂ at 37 °C). After 7 days, cells were harvested and stained for viability with LIVE/DEAD reagent (Invitrogen, Carlsbad, CA, USA), and the surface stained to measure CD56+CD3⁻ NK cells as described above. Data were finally reported as %NK cell proliferation, NK count, and % highly proliferating NK cells. Since the CellTrace Assay measures cycles of proliferation, % highly proliferating NK cells were defined as the percentage of NK cells that underwent 3 or more cycles of division.

2.5. In Vivo Mouse Study and Imaging

In order to establish efficacy of cam1615BCMA in vivo, we modified a previously described scid/hu model [20]. The MM.1S cell line was transfected with a luciferase reporter gene, and stable transfectants were cloned, allowing for weekly imaging in real time of each cancerous mouse. Briefly, NSG mice (NOD.Cg-Prkdc^{scid} Il2rg^{tm1Wjl}/SzJ, *n* = 6/group) were injected IP with 7.5×10^5 MM.1S-luc cells and then three days later conditioned with low-dose total body irradiation (275 cGy) to enhance NK cell engraftment. The following day, all groups received enriched NK cells, prepared by magnetically depleting PBMC of CD3⁺ and CD19⁺ cells, and TriKE treatment was initiated. A course of treatment consisted of 50 μ g of the drug given IP five times per week (MTWThF) for two weeks and then maintenance therapy three times per week (MWF). For weekly image sessions, mice were injected with 100 μ L of 30 mg/mL luciferin substrate 10 min prior to imaging under isoflurane gas sedation. Weekly imaging was performed using the Xenogen Ivis 100 imaging system with Living Image 2.5 analyzation software (Xenogen Corporation, Hopkington, MA, USA) at the University of Minnesota Imaging Center. A second experiment was performed for reproducibility. Mice were weighed weekly when possible. Animal studies were conducted in accordance with the Institutional Animal Care and Use Committee at the University of Minnesota (IACUC# 1909-37416A). The metastatic nature and ferocity of our MM.1S-luc model is illustrated in Supplemental Figure S3.

2.6. Statistical Analysis

For in vitro studies, GraphPad Prism (GraphPad Prism Software, Inc., La Jolla, CA, USA) was used to calculate differences via one-way ANOVA with repeated measures or paired t-test methods (as indicated) and to generate graphs with error bars showing the

mean \pm SEM and statistical significance. For in vivo mouse studies, the Kruskal–Wallis test with a Dunn’s Multiple Comparison post-test was employed. The Kruskal–Wallis test is a nonparametric test that compares the means of three or more unmatched groups. Data were expressed as median \pm IQR. p values less than 0.05 were considered significant.

3. Results

3.1. Construction of cam1615BCMA TriKE

The second generation cam1615BCMA, composed of a VHH camelid fragment recognizing CD16 fused with human IL-15 moiety and humanized anti-BCMA scFv antibody, was constructed using recombinant techniques, and the protein was expressed in a bacterial system. Figure 1A,B are expression vectors for cam1615BCMA showing different permutations of the anti-BCMA scFv, cam1615BCMAVHVL, and cam1615BCMAVLVH, respectively. The constructs are essentially the same, except the VH and VL genes encoding the anti-BCMA gene have been reversed. Figure 1C shows the absorbance tracing from the fast flow Q (FFQ) ion exchange column as the first phase of purification. The first sharp peak was collected, pooled, concentrated, and then passed over a second size exclusion column. Eluant was collected in 8 mL aliquots indicated on the abscissa of the graph. Figure 1D shows the absorbance tracing from the second phase of purification and size-exclusion chromatography (SEC). Each of the aliquots was analyzed using SDS-PAGE with Simply Blue Safe Stain to pinpoint fractions containing the target protein (Figure 1E). Fractions C5–C11 were combined into a pooled product and then analyzed again using SDS-PAGE (Figure 1F). The final result indicated a uniform product with purity greater than 90% by gel analysis.

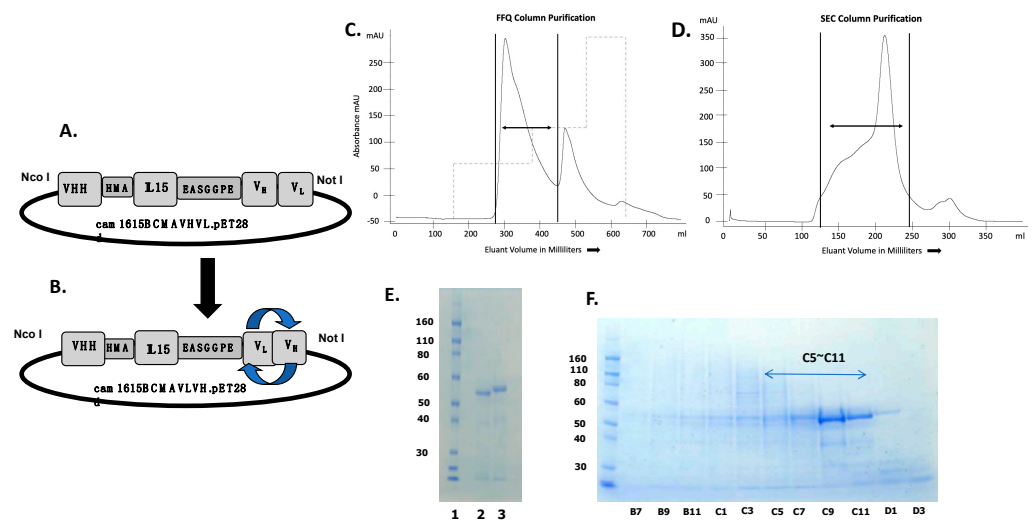


Figure 1. The construction of anti-BCMA trispecific killer engager (TriKE) cam1615BCMA. (A,B) are expression vectors comprising a VHH camelid fragment recognizing CD16 fused with human IL-15 and reversed permutations of the VH- and VL-encoding anti-BCMA gene, cam1615BCMAVHVL and cam1615BCMAVLVH, respectively. (C) Chromatography tracing from the fast flow Q (FFQ) ion exchange column as the first phase of purification. Dual arrows are collected peaks. (D) Chromatography tracing from the second phase of purification and size-exclusion chromatography (SEC). The first sharp FFQ peak was collected and then passed over a size-exclusion column. Eluant was collected in 8 mL aliquots indicated on the abscissa of the graph. (E) Each of the aliquots was analyzed with SDS-PAGE and Simply Blue Safe Stain. (F) Fractions C5–C11 were pooled and then analyzed.

3.2. cam1615BCMA TriKE Cytotoxicity Is Dose Dependent

The NK cell degranulation and IFN- γ production mediated by cam1615BCMA against MM.1S multiple myeloma cells at different drug doses are shown in Figure 2A,B. Figure 2A shows that CD107a levels were significantly elevated in mixtures of PBMC and MM.1S target cells treated with cam1615BCMA VHVL ($p = 0.0172$) and cam1615BCMA VLVH ($p < 0.0387$)

when compared to the no-treatment, IL15 monomer, and CAM16 monomer controls at a dose of 5 nM. An increase in IFN- γ levels was also observed with this same concentration of drug. Figure 2B shows an overall increase in CD107a levels in cam1615BCMA VHVL ($p = 0.0243$) and cam1615BCMA VLVH ($p = 0.0250$) compared to the controls at the higher dose of 30 nM. IFN- γ levels followed a similar pattern of response. Together, the data show that higher doses of TriKE results in higher activity, and there is little difference when the VL and VH regions are reversed on the construct.

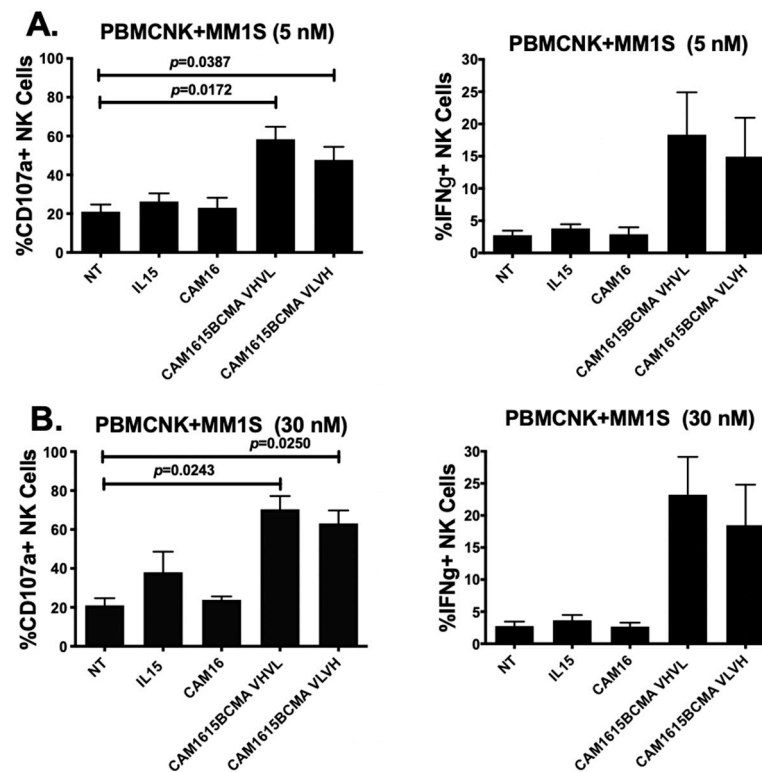


Figure 2. cam1615BCMA TriKE cytotoxicity is dose-dependent. In order to compare the effects of different concentrations of cam1615BCMA against a BCMA-positive multiple myeloma (MM) cell line, peripheral blood mononuclear cells (PBMCs) were incubated with BCMA-positive MM.1S target cells overnight then incubated with 5 nM or 30 nM of cam1615BCMA and controls. Cells were then washed, stained, and fixed for flow cytometric evaluation. CD107a degranulation activity (left) and IFN- γ production (right) of the effector and target cell mixture treated with cam1615BCMA VHVL and cam1615BCMA VLVH were compared to the no-treatment (NT), IL15 monomer, and cam16 monomer controls at (A) 5 nM and at (B) 30 nM equimolar concentrations of reagent. Significant values were determined using one-way Anova testing with repeated measures to calculate differences against the no-treatment (NT) control.

3.3. cam1615BCMA TriKE Is Cytotoxic against Various Multiple Myeloma Targets

NK activity and IFN- γ activity of cam1615BCMA TriKE were tested on PBMCs alone and PBMC against three human multiple myeloma target cell lines in Figure 3A–D. Figure 3A shows the PBMC only with no cancer cells added as background controls. In Figure 3B, both cam1615BCMA TriKE and Daratumumab resulted in significantly higher NK cell CD107a levels against MM.1S cells when analyzed using Student's *t* test. Only the Daratumumab group was significant using one-way ANOVA analysis. cam1615BCMA TriKE also elevated IFN- γ levels more than both cam161519 TriKE and Daratumumab.

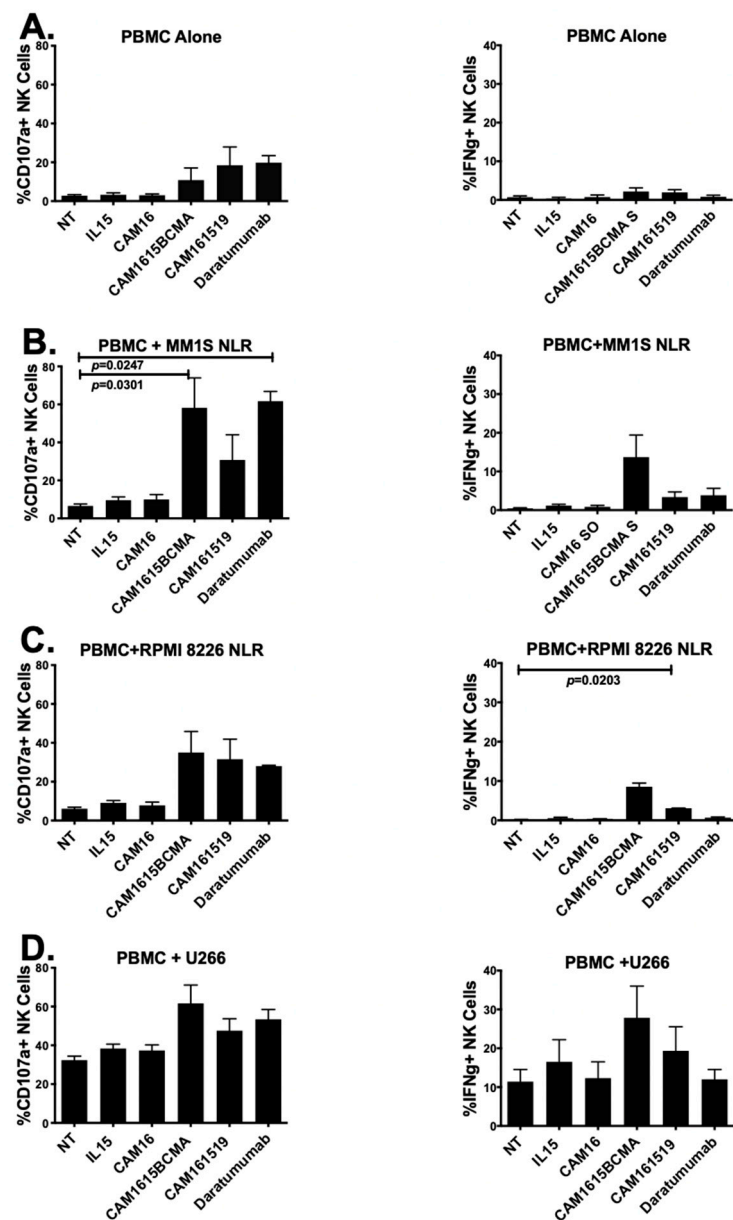


Figure 3. cam1615BCMA TriKE is cytotoxic against various multiple myeloma targets. In order to determine the cytotoxicity of cam1615BCMA, PBMCs incubated with BCMA-positive MM target cells were incubated with cam1615BCMA TriKE, cam161519 TriKE, Daratumumab, and monomeric controls. Cells were then washed, stained, and fixed for flow cytometric evaluation. CD107a levels (left) and IFN- γ levels (right) were measured with (A) PBMC effector cells alone, (B) PBMCs with MM.1S target cells, (C) PBMCs with RPMI 8226 target cells, and (D) PBMCs with U266 target cells. Significant values were determined using one-way ANOVA testing and Student’s t test in comparison to the no-treatment (NT) control.

cam161519 was used as a negative control since CD19 is known to be expressed in lower levels on this cell line. Figure 3C shows that cam1615BCMA TriKE was associated with a greater increase in NK cell CD107a levels than both cam161519 and Daratumumab and significantly elevated IFN- γ levels ($p = 0.0203$), compared to the NT, against RPMI 8226 target cells. Figure 3D shows that cam1615BCMA TriKE and Daratumumab both increase NK cell CD107a levels compared to the NT against U266 cells. While cam1615BCMA TriKE elevated NK cell IFN- γ levels more than both cam161519 and Daratumumab in a co-culture of PBMCs and U266 target cells, the background activity against this cell line was higher.

Because the CD107a assay used in these experiments provides an indirect measure of NK cytotoxicity, a 51 chromium release assay was also performed to measure tumor killing (Table 1). Upon cytotoxicity of target cells, CD107a-containing intracytoplasmic granule membranes from normal NK cells fuse with the outer NK-cell membrane, resulting in detectable surface CD107a expression and providing the basis of the CD107a assay. The 51 chromium release assay is based on the release of isotope from labeled target cells upon their lysis by NK cells. In our 51 chromium release assay, when NK effector cells were incubated with labeled MM1.S target cells, treatment with cam1615BCMA TriKE lysed about 39%, 20%, and 10% of MM1.S labeled targets at effector:target cell ratios of 20:1, 6.6:1, and 2.2:1, respectively. In contrast, no target lysis was detected in control samples treated with anti-CD16 alone, anti-BCMA alone, IL-15 alone, or no treatment. Thus, the 51 chromium functional study confirms our use of CD107a assay as a measure of NK cell killing and function.

Table 1. cam1615BCMA increases cytotoxicity of MM.1S target cells as measured by 51 chromium release *.

Treatment	Effector: Target Ratio		
	20:1	6.6:1	2.2:1
no treatment	0.0	0.2	0.0
cam1615BCMA	38.7	20.0	10.3
IL15 alone	0.1	0.0	0.0
anti-cam16 alone	0.0	0.0	0.0
anti-BCMA alone	0.2	0.0	0.0

* Data are presented as % 51 chromium release. Standard deviations did not exceed 18% of the mean.

3.4. cam1615BCMA TriKE Induces Specific NK Cell Proliferation

To verify the potency of the IL-15 moiety cross-linked in the TriKE, an expansion analysis was performed. Figure 4A,C shows that cam1615BCMA TriKE increased NK cell proliferation and elevated highly proliferated NK cell populations significantly better than the no-treatment control (NT). Figure 4B shows that cam1615BCMA also increased the raw number of NK cells relative to the NT. Furthermore, the IL-15 linker in cam1615BCMA had comparable effects to the IL-15 monomer on the proliferation of NK cells. Figure 4D–F shows that while the IL-15 monomer increases T cell proliferation and highly proliferated populations, cam1615BCMA does not have the same effect as it did in NK cells. The IL-15 linker in cam1615BCMA therefore specifically induces NK cell proliferation and does not induce T cell proliferation.

3.5. In Vivo Efficacy of cam1615BCMA TriKE

To evaluate TriKE efficacy, an MM mouse xenograft model was developed in which both human MM cells and human NK cells were engrafted. Figure 5A,B shows the imaging results of the mice in the treatment and no-treatment groups, respectively. The in vivo data visually and qualitatively showed that mouse tumors were larger and more prevalent in the no-treatment group than in the treatment group. The cam1615BCMA TriKE induced minimal weight change in mice through the first 31 days, alluding to safety in the profile of this drug (Figure 5C). Figure 5D is the total tumor bioluminescence (total flux) of the mice in each treatment group 18 days after they were grafted with MM.1S-luc cells that showed cam1615BCMA inhibited tumor growth better than the no-treatment (NT) negative control ($p < 0.05$). Figure 5E is the total flux of the mice in each treatment group 31 days after tumor administration, which showed an even greater difference between these two groups. This difference, a robust trend in tumor decrease ($p = 0.066$ by Kruskal–Wallis analysis) is impacted by a single outlier in the cam1615BCMA group that could be explained by lack of NK cell engraftment in that mouse due to technical error. If the single outlier is removed from the cam1615BCMA group on day 31, the p value equals 0.0219.

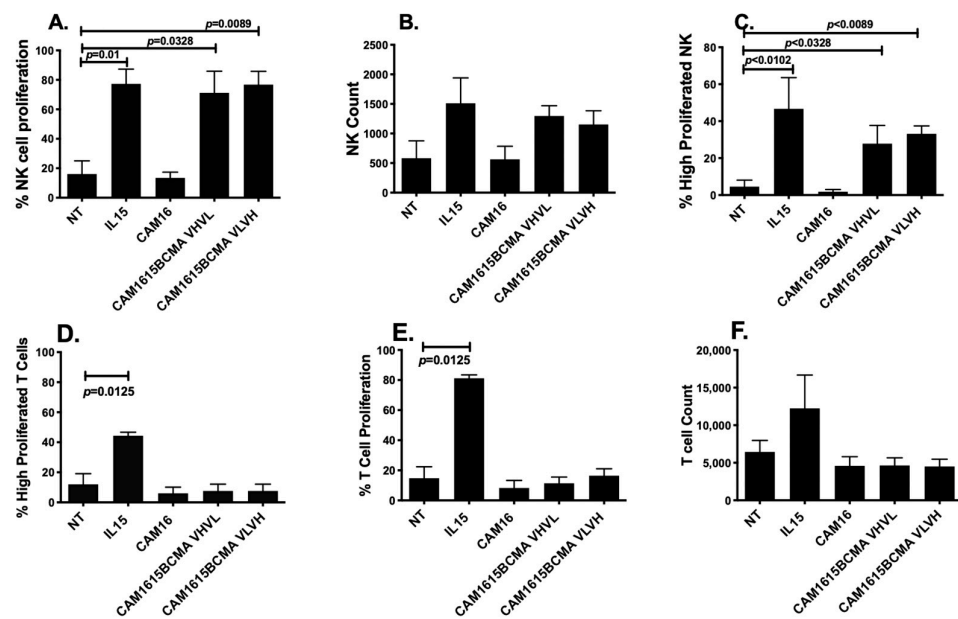


Figure 4. cam1615BCMA TriKE induces NK cell proliferation. To verify the potency of the IL-15 moiety cross-linked in the TriKE, PBMCs were labeled with CellTrace Violet and incubated for seven days with 5 nM of IL-15 or cam1615BCMA. After seven days, the cells were harvested and stained for flow cytometric evaluation. (A) The percentage of total NK cells that proliferated, (B) the raw number of NK cells, and (C) the percentage of total NK cells that proliferated three or more divisions because of each treatment were counted. Similarly, (D) the percentage of total T cells that proliferated, (E) the raw number of T cells, and (F) the percentage of total T cells that proliferated three or more divisions because of each treatment were also counted. Significant values were determined using one-way ANOVA with repeated measures against the no-treatment (NT) control.

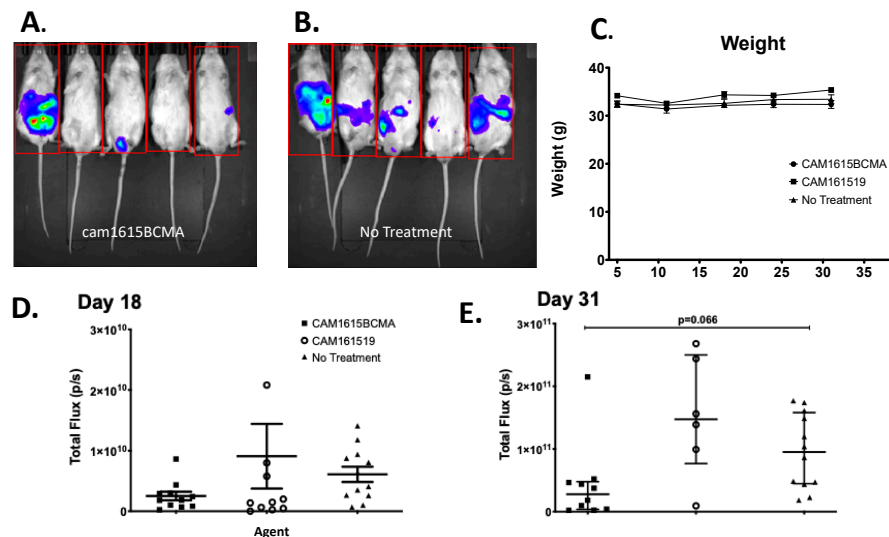


Figure 5. In vivo efficacy of cam1615BCMA TriKE. To evaluate TriKE efficacy, both human MM cells and human NK cells were engrafted in a MM mouse xenograft model. Mice received IP injections of MM.1S-luc cells followed by enriched NK cells and received cam1615BCMA TriKE, cam161519, or no-treatment (NT) control. Bioluminescent imaging measured total flux radiance (p/s) of MM.1S tumor in mice treated with (A) cam1615BCMA (N = 5) and (B) no treatment (N = 6) on day 33. (C) Weekly average weights over the 31 days of treatment in each treatment group were recorded to monitor mouse health. The total tumor bioluminescence (total flux) of each mouse in each treatment group was represented as points on a scatter plot for (D) day 18 and (E) day 31. For data analysis, the Kruskal–Wallis test with a Dunn’s Multiple Comparison post-test was employed. Red box indicates region of interest.

4. Discussion

This work shows for the first time that (1) BCMA is a valid target for NK cell-mediated ADCC when targeted with a TriKE; (2) BCMA expressing MM.1S tumor can be controlled *in vivo* in a murine xenograft model with enhanced NK engagement by cam1615BCMA; (3) the drug can be safely used *in vivo* with minimal toxicity despite the presence of an IL-15 cross-linker; and (4) cam1615BCMA induces potent NK cell proliferation without inducing T cell proliferation.

Recent clinical breakthroughs in BCMA-targeting therapeutics include the anti-BCMA antibody drug conjugate belantamab mafodotin (blmf), the BCMA \times CD3 bispecific T cell engager (BiTE) teclistamab, and BCMA-directed CAR T therapies (NCT02064387, NCT03145181, NCT03090659, NCT03318861, NCT02215967, NCT03548207, and NCT04133636). Despite these advancements, T cells may cause cytokine release storm (CRS). CAR T cell and BiTE therapies have been shown to induce CRS resulting in cytokine toxicity and neurotoxicity [12,13]. Furthermore, only the patient's autologous T cells can be used for CAR T because of major histocompatibility complex (MHC) restrictions. The risk of CRS is drastically reduced in NK cells, which are broadly triggered by malignant tumor cells and virally infected cells with reduced or absent expression of MHC I [35].

Organisms from the family Camelidae naturally possess sdAbs that lack light chains. Because of the absence of light chains, camelid antibodies have smaller antigen-binding surface areas and a simplified design which is optimal for engineering and cloning drugs requiring antibody fragments [18]. The effectiveness of first-generation TriKEs with multiple scFv components resulted in the aggregation of the anti-CD16 scFv and the TAA scFv in the refolding process [22,23]. To circumvent this refolding problem, the complementarity-determining regions (CDR), or the binding regions of an antibody that determine antigen specificity, from a camelid anti-CD16 sdAb were cloned into a humanized sdAb backbone [31]. Based on the aforementioned molecular improvements, our research group generated the anti-CD16 molecule known as cam16 that was used in the construction of the second-generation camelized drug called cam1615BCMA.

We compared cam1615BCMA VHVL and cam1615BCMA VLVH in order to determine if reversing the VH-VL domain orientation on the BCMA scFv would impact ADCC, cytokine production, or NK cell proliferation. Reversing VH-VL domain orientation has been found to enhance bacterial expression and increase scFv production yield without impairing *in vitro* and *in vivo* binding [36]. Our laboratory previously found that shuffling the orientation of the VH-VL domains of a bispecific immunotoxin actually improved the efficacy of the reagent against B cell lymphoma [37]. However, we found there was no significant difference between the *in vitro* effectiveness of cam1615BCMA VHVL and cam1615BCMA VLVH in inducing degranulation, interferon gamma production, or NK cell proliferation.

CD16 activation in NK cells mediates ADCC which results in NK cell degranulation targeted towards the tumor. However, the CD16 receptor undergoes rapid downregulation via disintegrin and metalloproteinase-17 (ADAM17)-regulated cleavage following NK cell activation [38], a process which might pose a limitation to TriKE function. Inhibiting ADAM17 downregulation could increase CD16 signaling and thus enhance sustained ADCC activity. ADAM17 checkpoint inhibitors used in combination with BiKEs have already shown promise in enhancing NK activation, which supports the therapeutic potential for using ADAM17 checkpoint inhibitors in combination with NK cell engagers targeting CD16 [39].

Though CD16 induces NK activation and cytokine signaling, it cannot induce NK proliferation without IL-15 signaling [40]. Both IL-2 and IL-15 signaling triggers the proliferation of cytotoxic T cells and NK cells upon binding to the IL-2/IL-15 cytokine receptor; however, IL-15 signaling does not maintain regulatory T cells (Tregs) as IL-2 signaling does [41,42]. Interestingly, we found that cam1615BCMA induced significantly higher levels of only NK cell proliferation compared to the no-treatment controls, while free IL-15 induced significantly higher levels of both NK cell and T cell proliferation. The absence

of T cell proliferation induced by cam1615BCMA suggests that the mechanism by which the IL-15 linker in the TriKE induces NK cell proliferation is highly selective and possibly dependent on cam16 binding to CD16. NK cell engagers could prove useful for future clinical study because it raises the possibility of combining TriKEs with T cell therapeutics for a two-pronged immunotherapy approach. Preclinical studies with continuous intravenous infusion of free IL-15 have shown severe dose-limiting toxicity [43]. Subcutaneous administration of cam1615BCMA may enhance drug delivery by further reducing IL-15 toxicity and thereby increasing the maximum tolerated dose of the drug [44]. We investigated weight loss in mice as a measure of toxicity because it precludes death and, because we did not observe weight loss in the mice, our preclinical data indicate that cam1615BCMA is not toxic in vivo within our model system. NSG mice are not an optimal model for studying toxicity. Thus, further investigation will be required to fully characterize the toxicity profile of cam1615BCMA. Still, data suggest the IL-15 linker in cam1615BCMA lacks the off-target T cell stimulation associated with free IL-15.

5. Conclusions

We have described a novel NK cell-engaging complex that induces ADCC and cytokine signaling in multiple myeloma in vitro. cam1615BCMA selectively induces the proliferation of NK cells without stimulating T cells in vitro and has shown to be both safe and effective in a mouse xenograft model. Taken together, these findings suggest that B-cell leukemia and lymphoma may be relevant therapeutic targets for cam1615BCMA in the future. Based on our preclinical findings, cam1615BCMA is a promising immunotherapeutic candidate for clinical trials and deserves consideration moving forward.

Supplementary Materials: The following supporting information can be downloaded at <https://www.mdpi.com/article/10.3390/immuno3020016/s1>, Figure S1: TriKe Mechanism of Action; Figure S2: Representative gating strategy; Figure S3: MM.1S tumor progression is aggressive in vivo.

Author Contributions: Conceptualization, F.O., D.A.V., J.S.M. and M.F.; visualization, B.K.; formal analysis, B.K. and M.F.; funding acquisition, D.A.V.; resources, D.A.V., J.S.M. and M.F.; validation, J.S.M.; writing—original draft, D.A.V. and F.O.; writing—review and editing, D.A.V., J.S.M. and M.F.; All authors have read and agreed to the published version of the manuscript.

Funding: This work was supported in part by US Public Health Service Grant R01-CA72669, P01-CA65493, P01-CA111412, R35 CA197292, R03-CA2-31766, R03-CA2-16114, 2T32HL007062 Hematology Research Training Program T32 at the University of Minnesota, and P30 CA077598 awarded by the NCI and the NIAID, DHHS. It was also supported by the Randy Shaver Cancer Research and Community Fund, Cancer Center, Minnesota Masonic Charities, the Osteosarcoma Institute, and the Sarcoma Foundation of America.

Institutional Review Board Statement: The study was conducted in accordance with the Declaration of Helsinki and approved by the IACUC of the University of Minnesota (protocol# 2209-40433A and approval date February 2022).

Informed Consent Statement: Informed consent was obtained. Peripheral blood mononuclear cells (PBMCs) from the blood of de-identified healthy donors were obtained, after participants gave informed consent, from Memorial Blood Centers (Minneapolis, MN, USA) and used in compliance with the Committee on the Use of Human Subjects in Research (IRB# 9709M00134) and in accordance with the Declaration of Helsinki.

Data Availability Statement: The raw data supporting the conclusions of this article will be made available by the authors.

Acknowledgments: We would like to acknowledge the Translational Therapy Laboratory, Flow Cytometry, and Imaging cores at the University of Minnesota for their excellent services.

Conflicts of Interest: Vallera, Felices, and Miller receive research support and, with the University of Minnesota, are shared owners of the TriKE technology licensed by the University to GT Biopharma, Inc. This relationship has been reviewed and managed by the University of Minnesota in accordance with its conflict of interest policies.

References

1. Cowan, A.J.; Green, D.J.; Kwok, M.; Lee, S.; Coffey, D.G.; Holmberg, L.A.; Tuazon, S.; Gopal, A.K.; Libby, E.N. Diagnosis and Management of Multiple Myeloma: A Review. *JAMA* **2022**, *327*, 464–477. [[CrossRef](#)] [[PubMed](#)]
2. Mian, H.; Eisfeld, C.; Venner, C.P.; Masih-Khan, E.; Kardjadj, M.; Jimenez-Zepeda, V.H.; Khandanpour, C.; Lenz, G.; McCurdy, A.; Sebag, M.; et al. Efficacy of Daratumumab-Containing Regimens Among Patients With Multiple Myeloma Progressing on Lenalidomide Maintenance: Retrospective Analysis. *Front. Oncol.* **2022**, *12*, 826342. [[CrossRef](#)]
3. Swan, D.; Routledge, D.; Harrison, S. The evolving status of immunotherapies in multiple myeloma: The future role of bispecific antibodies. *Br. J. Haematol.* **2022**, *196*, 488–506. [[CrossRef](#)] [[PubMed](#)]
4. Steinmetz, H.T.; Singh, M.; Milce, J.; Haidar, M.; Rieth, A.; Lebioda, A.; Kohnke, J. Management of Patients with Relapsed and/or Refractory Multiple Myeloma Treated with Novel Combination Therapies in Routine Clinical Practice in Germany. *Adv. Ther.* **2022**, *39*, 1247–1266. [[CrossRef](#)] [[PubMed](#)]
5. Kumar, S.K.; Dimopoulos, M.A.; Kastiris, E.; Terpos, E.; Nahi, H.; Goldschmidt, H.; Hillengass, J.; Leleu, X.; Beksac, M.; Alsina, M.; et al. Natural history of relapsed myeloma, refractory to immunomodulatory drugs and proteasome inhibitors: A multicenter IMWG study. *Leukemia* **2017**, *31*, 2443–2448. [[CrossRef](#)]
6. Shah, N.; Chari, A.; Scott, E.; Mezzi, K.; Usmani, S.Z. B-cell maturation antigen (BCMA) in multiple myeloma: Rationale for targeting and current therapeutic approaches. *Leukemia* **2020**, *34*, 985–1005. [[CrossRef](#)]
7. Lee, L.; Bounds, D.; Paterson, J.; Herledan, G.; Sully, K.; Seestaller-Wehr, L.M.; Fieles, W.E.; Tunstead, J.; McCahon, L.; Germaschewski, F.M.; et al. Evaluation of B cell maturation antigen as a target for antibody drug conjugate mediated cytotoxicity in multiple myeloma. *Br. J. Haematol.* **2016**, *174*, 911–922. [[CrossRef](#)] [[PubMed](#)]
8. Eckhert, E.; Hewitt, R.; Liedtke, M. B-cell maturation antigen directed monoclonal antibody therapies for multiple myeloma. *Immunotherapy* **2019**, *11*, 801–811. [[CrossRef](#)]
9. Tai, Y.T.; Acharya, C.; An, G.; Moschetta, M.; Zhong, M.Y.; Feng, X.; Cea, M.; Cagnetta, A.; Wen, K.; van Eenennaam, H.; et al. APRIL and BCMA promote human multiple myeloma growth and immunosuppression in the bone marrow microenvironment. *Blood* **2016**, *127*, 3225–3236. [[CrossRef](#)]
10. Darce, J.R.; Arendt, B.K.; Wu, X.; Jelinek, D.F. Regulated expression of BAFF-binding receptors during human B cell differentiation. *J. Immunol.* **2007**, *179*, 7276–7286. [[CrossRef](#)]
11. Palumbo, A.; Anderson, K. Multiple myeloma. *N. Engl. J. Med.* **2011**, *364*, 1046–1060. [[CrossRef](#)]
12. Teachey, D.T.; Rheingold, S.R.; Maude, S.L.; Zugmaier, G.; Barrett, D.M.; Seif, A.E.; Nichols, K.E.; Suppa, E.K.; Kalos, M.; Berg, R.A.; et al. Cytokine release syndrome after blinatumomab treatment related to abnormal macrophage activation and ameliorated with cytokine-directed therapy. *Blood* **2013**, *121*, 5154–5157. [[CrossRef](#)]
13. Shimabukuro-Vornhagen, A.; Gödel, P.; Subklewe, M.; Stemmler, H.J.; Schlößer, H.A.; Schlaak, M.; Kochanek, M.; Boll, B.; von Bergwelt-Baildon, M.S. Cytokine release syndrome. *J. Immunother. Cancer* **2018**, *6*, 56. [[CrossRef](#)]
14. Myers, J.A.; Miller, J.S. Exploring the NK cell platform for cancer immunotherapy. *Nat. Rev. Clin. Oncol.* **2021**, *18*, 85–100. [[CrossRef](#)]
15. Lanier, L.L.; Ruitenberg, J.J.; Phillips, J.H. Functional and biochemical analysis of CD16 antigen on natural killer cells and granulocytes. *J. Immunol.* **1988**, *141*, 3478–3485. [[CrossRef](#)]
16. Yokoyama, W.M.; Plougastel, B.F. Immune functions encoded by the natural killer gene complex. *Nat. Rev. Immunol.* **2003**, *3*, 304–316. [[CrossRef](#)] [[PubMed](#)]
17. Lanier, L.L. Natural killer cell receptor signaling. *Curr. Opin. Immunol.* **2003**, *15*, 308–314. [[CrossRef](#)] [[PubMed](#)]
18. Muyldermans, S. Nanobodies: Natural single-domain antibodies. *Annu. Rev. Biochem.* **2013**, *82*, 775–797. [[CrossRef](#)] [[PubMed](#)]
19. Felices, M.; Lenvik, T.; Kodal, B.; Lenvik, A.; Hinderlie, P.; Bendzick, L.; Schirm, D.; Kaminski, M.; McElmurry, R.; Geller, M.; et al. Potent Cytolytic Activity and Specific IL15 Delivery in a Second-Generation Trispecific Killer Engager. *Cancer Immunol. Res.* **2020**, *8*, 1139–1149. [[CrossRef](#)]
20. Vallera, D.A.; Oh, F.; Kodal, B.; Hinderlie, P.; Geller, M.A.; Miller, J.S.; Felices, M. A HER2 Tri-Specific NK Cell Engager Mediates Efficient Targeting of Human Ovarian Cancer. *Cancers* **2021**, *8*, 3994. [[CrossRef](#)]
21. Vallera, D.A.; Ferrone, S.; Kodal, B.; Hinderlie, P.; Bendzick, L.; Ettestad, B.; Hallstrom, C.; Zorko, N.A.; Rao, A.; Fujioka, N.; et al. NK-Cell-Mediated Targeting of Various Solid Tumors Using a B7-H3 Tri-Specific Killer Engager In Vitro and In Vivo. *Cancers* **2020**, *12*, 2659. [[CrossRef](#)]
22. Schmohl, J.U.; Felices, M.; Taras, E.; Miller, J.S.; Vallera, D.A. Enhanced ADCC and NK Cell Activation of an Anticarcinoma Bispecific Antibody by Genetic Insertion of a Modified IL-15 Cross-linker. *Mol. Ther.* **2016**, *24*, 1312–1322. [[CrossRef](#)] [[PubMed](#)]
23. Vallera, D.A.; Felices, M.; McElmurry, R.; McCullar, V.; Zhou, X.; Schmohl, J.U.; Zhang, B.; Lenvik, A.J.L.; Panoskaltis-Mortari, A.; Verneris, M.R.; et al. IL15 Trispecific Killer Engagers (TriKE) Make Natural Killer Cells Specific to CD33+ Targets While Also Inducing Persistence, In Vivo Expansion, and Enhanced Function. *Clin. Cancer Res.* **2016**, *22*, 3440–3450. [[CrossRef](#)]
24. Steel, J.C.; Waldmann, T.A.; Morris, J.C. Interleukin-15 biology and its therapeutic implications in cancer. *Trends Pharmacol. Sci.* **2012**, *33*, 35–41. [[CrossRef](#)] [[PubMed](#)]
25. Carson, W.E.; Giri, J.G.; Lindemann, M.J.; Linett, M.L.; Ahdieh, M.; Paxton, R.; Anderson, D.; Eisenmann, J.; Grabstein, K.; Caligiuri, M.A. Interleukin (IL) 15 is a novel cytokine that activates human natural killer cells via components of the IL-2 receptor. *J. Exp. Med.* **1994**, *180*, 1395–1403. [[CrossRef](#)]

26. Zhang, Y.; Wallace, D.L.; De Lara, C.M.; Ghattas, H.; Asquith, B.; Worth, A.; Griffin, G.E.; Taylor, G.P.; Tough, D.F.; Beverley, P.C.L.; et al. In vivo kinetics of human natural killer cells: The effects of aging and acute and chronic viral infection. *Immunology* **2007**, *121*, 258–265. [[CrossRef](#)]
27. Berger, S.C.; Berger, M.; Hackman, R.C.; Gough, M.; Elliott, C.; Jensen, M.C.; Riddell, S.R. Safety and immunologic effects of IL-15 administration in nonhuman primates. *Blood* **2009**, *114*, 2417–2426. [[CrossRef](#)] [[PubMed](#)]
28. Munger, W.; Dejoy, S.Q.; Jeyaseelan, R.; Torley, L.W.; Grabstein, K.H.; Eisenmann, J.; Paxton, R.; Cox, T.; Wick, M.M.; Kerwar, S.S. Studies evaluating the antitumor activity and toxicity of interleukin-15, a new T cell growth factor: Comparison with interleukin-2. *Cell. Immunol.* **1995**, *165*, 289–293. [[CrossRef](#)]
29. Behar, G.; Siberil, S.; Groulet, A.; Chames, P.; Pugniere, M.; Boix, C.; Sautes-Fridman, C.; Teillaud, J.L.; Baty, D. Isolation and characterization of anti-Fcγ₃ (CD16) llama single-domain antibodies that activate natural killer cells. *Protein Eng. Des. Sel.* **2008**, *21*, 1–10. [[CrossRef](#)]
30. Cohen, A.D.; Garfall, A.L.; Stadtmauer, E.A.; Melenhorst, J.J.; Lacey, S.F.; Lancaster, E.; Vogl, D.T.; Weiss, B.M.; Dengel, K.; Nelson, A.; et al. B cell maturation antigen-specific CAR T cells are clinically active in multiple myeloma. *J. Clin. Investig.* **2019**, *129*, 2210–2221. [[CrossRef](#)]
31. Vincke, C.; Loris, R.; Saerens, D.; Martinez-Rodriguez, S.; Muyldermans, S.; Conrath, K. General strategy to humanize a camelid single-domain antibody and identification of a universal humanized nanobody scaffold. *J. Biol. Chem.* **2009**, *284*, 3273–3284. [[CrossRef](#)] [[PubMed](#)]
32. Vallera, D.A.; Todhunter, D.; Kuroki, D.W.; Shu, Y.; Sicheneder, A.; Panoskaltis-Mortari, A.; Vallera, V.D.; Chen, H. Molecular modification of a recombinant, bivalent anti-human CD3 immunotoxin (Bic3) results in reduced in vivo toxicity in mice. *Leuk. Res.* **2005**, *29*, 331–341. [[CrossRef](#)] [[PubMed](#)]
33. Eskelinen, E.L. Roles of LAMP-1 and LAMP-2 in lysosome biogenesis and autophagy. *Mol. Asp. Med.* **2006**, *27*, 495–502. [[CrossRef](#)] [[PubMed](#)]
34. Zaritskaya, L.; Shurin, M.R.; Sayers, T.J.; Malyguine, A.M. New flow cytometric assays for monitoring cell-mediated cytotoxicity. *Expert Rev. Vaccines* **2010**, *9*, 601–616. [[CrossRef](#)]
35. Lowdell, M.W.; Lamb, L.; Hoyle, C.; Velardi, A.; Prentice, H.G. Non-MHC-restricted cytotoxic cells: Their roles in the control and treatment of leukaemias. *Br. J. Haematol.* **2001**, *114*, 11–24. [[CrossRef](#)]
36. Hamilton, S.; Odili, J.; Gundogdu, O.; Wilson, G.D.; Kupsch, J.M. Improved production by domain inversion of single-chain Fv antibody fragment against high molecular weight proteoglycan for the radioimmunotargeting of melanoma. *Hybrid. Hybridomics* **2001**, *20*, 351–360. [[CrossRef](#)]
37. Vallera, D.A.; Chen, H.; Sicheneder, A.R.; Panoskaltis-Mortari, A.; Taras, E.P. Genetic alteration of a bispecific ligand-directed toxin targeting human CD19 and CD22 receptors resulting in improved efficacy against systemic B cell malignancy. *Leuk. Res.* **2009**, *33*, 1233–1242. [[CrossRef](#)]
38. Romee, R.; Foley, B.; Lenvik, T.; Wang, Y.; Zhang, B.; Ankarlo, D.; Luo, X.; Cooley, S.; Verneris, M.; Walcheck, B.; et al. NK cell CD16 surface expression and function is regulated by a disintegrin and metalloprotease-17 (ADAM17). *Blood* **2013**, *121*, 2599–3608. [[CrossRef](#)]
39. Wiernik, A.; Foley, B.; Zhang, B.; Verneris, M.R.; Warlick, E.; Gleason, M.K.; Ross, J.A.; Luo, X.; Weisdorf, D.J.; Walcheck, B.; et al. Targeting natural killer cells to acute myeloid leukemia in vitro with a CD16×33 bispecific killer cell engager and ADAM17 inhibition. *Clin. Cancer Res.* **2013**, *19*, 3844–3855. [[CrossRef](#)]
40. Ali, A.K.; Nandagopal, N.; Lee, S.H. IL-15-PI3K-AKT-mTOR: A critical pathway in the life journey of Natural Killer cells. *Front. Immunol.* **2015**, *6*, 355. [[CrossRef](#)] [[PubMed](#)]
41. Sarhan, D.; Brandt, L.; Felices, M.; Guldevall, K.; Lenvik, T.; Hinderlie, P.; Curtsinger, J.; Warlick, E.; Spellman, S.R.; Blazar, B.R.; et al. 161533 TriKE stimulates NK-cell function to overcome myeloid-derived suppressor cells in MDS. *Blood Adv.* **2018**, *2*, 1459–1469. [[CrossRef](#)] [[PubMed](#)]
42. Waldmann, T.A. The biology of interleukin-2 and interleukin-15: Implications for cancer therapy and vaccine design. *Nat. Rev. Immunol.* **2006**, *6*, 595–601. [[CrossRef](#)]
43. Sneller, M.C.; Kopp, W.C.; Engelke, K.J.; Yovandich, J.L.; Creekmore, S.P.; Waldmann, T.A.; Lane, H.C. IL-15 administered by continuous infusion to rhesus macaques induces massive expansion of CD8⁺ T effector memory population in peripheral blood. *Blood* **2011**, *118*, 6845–6848. [[CrossRef](#)] [[PubMed](#)]
44. Miller, J.S.; Morishima, C.; McNeel, D.G.; Patel, M.R.; Kohrt, H.E.K.; Thompson, J.A.; Sondel, P.M.; Wakelee, H.A.; Disis, M.L.; Kaiser, J.C.; et al. A first-in-human phase I study of subcutaneous outpatient recombinant human IL15 (rhIL15) in adults with advanced solid tumors. *Clin. Cancer Res.* **2018**, *24*, 1525–1535. [[CrossRef](#)] [[PubMed](#)]

Disclaimer/Publisher’s Note: The statements, opinions and data contained in all publications are solely those of the individual author(s) and contributor(s) and not of MDPI and/or the editor(s). MDPI and/or the editor(s) disclaim responsibility for any injury to people or property resulting from any ideas, methods, instructions or products referred to in the content.